Acoustic detection potential of single minimum ionising particles in noble liquids

Panos Oikonomou,* Laura Manenti,† Francesco Arneodo,‡ and Isaac Sarnoff
Division of Science, New York University Abu Dhabi, United Arab Emirates and
Center for Astro, Particle, and Planetary Physics (CAP^3),
New York University Abu Dhabi, United Arab Emirates
(Dated: July 11, 2022)

In an attempt to provide an additional detection channel for direct dark matter experiments involving noble liquid scintillators, we present a theoretical framework for describing the production of sound by single particles through noble liquids. We develop a linear classical description of the acoustic wave that accounts for viscous strong damping. We proceed with quantizing this description by introducing an effective field theory where we treat strong damping nonperurbatively through the introduction of an interaction between particles and antiparticles of sound. Throughout the paper, we use Minimum Ionizing Particles (MIPs) as a toy model to obtain quantitative results from our formalism.

CONTENTS

I. Introduction 1

II. Strongly Damped Acoustic Wave Equation 2
A. Damping Term Derivation 2
1. Derivation from Navier Stokes 2
2. Damping Characteristic 2
B. Source Term Derivation 3
1. Derivation from Navier Stokes 3
2. Low Viscosity Assumption 3

III. Analytic Solutions to the Wave Equation 3
A. Approximations Using Perturbation Theory 4
B. Green's Functions 4
1. Using Potentials and Residues 4
2. Properties of Residues 5
3. Calculation of Residues and Green's Functions 5
C. Causality 6
D. Closed Form solution for Delta Source 6
E. Sound sources for different particle speeds 6
1. Slow Particles 7
2. Fast Particles 7
F. Leading Order Analytic Solution 7

IV. Applications to MIPs 8
A. Energy Deposition Estimation 8
B. Numerical Estimates for Muon Signal in Different Media 9

V. Conclusion 10

References 11

* panoso@nyu.edu
† laura.manenti@nyu.edu
‡ francesco.arneodo@nyu.edu

I. INTRODUCTION

Research in the production of acoustic signals by charged particles received increasing attention after the characterization of acoustic waves produced by "local heating" in 1957 [1]. Local heating is considered to be the primary mechanism by which charged particles passing through liquids deposit energy in a way that gives rise to acoustic radiation [2]. At high incoming particle energies this signal is detectable, hence the acoustic signals of heavy ion beams, PeV particle cascades, or high energy neutrinos were heavily investigated between the 1960s and the early 1990s [3–9].

Acoustic detection has traditionally been used as a tool to detect high energy cosmic particles [10–12]. Yet recently, it has found applications in lower energies in the search for cold dark matter using superheated liquids [13–16]. Lowering the particle energy to the KeV range was achieved by detecting the shockwave produced during a local, instantaneous phase transition due to the particle's interaction in a superfluid medium [17]. This brilliant idea to lower particle energy, however, comes with the cost of having to conduct the experiment in a specialized thermodynamic state so that such nonlinear effects are observed.

In a liquid with not such finely controlled thermodynamical state, it is hard to theoretically calculate an estimate of the acoustic signal produced by lower energy particles. In such environments, apart from the lack of nonlinear effects such as molecular dissociation, microbubble formation, or shocks, [18] other effects such as viscosity decrease the validity of theoretical estimates at large distances [19].

In this study, the problem of estimating acoustic signals from single particles due to local heating is revisited and generalized in two ways. The first level of generalization is to consider arbitrary, moving, and compactly supported heat depositions (instead of specializing to local heating), allowing for our model to hold for alternative physical descriptions of acoustic production. Furthermore, a way to correct for the viscosity of the liquids is introduced, enabling more accurate estimates of the

signal attenuation at large distances from the particle track. Finally, the acoustic signal of relativistic muons is calculated as an application of this methodology. This paper further provides a detailed outline of the physical derivations needed in order to highlight any assumptions and be used as a resource for a general audience conducting feasibility studies for acoustic signals of particles in viscous liquids.

II. STRONGLY DAMPED ACOUSTIC WAVE EQUATION

We introduce the mechanism behind the generation of an acoustic signal due to a single particle interaction in a liquid. Let us first consider the effect of an arbitrary heat deposition in the bulk of the liquid. For this purpose, we add a source term and a damping term to the well-known acoustic wave equation in an isothermal fluid:

$$\Delta p(\boldsymbol{x},t) = \rho_0\kappa\frac{\partial^2}{\partial t^2}p(\boldsymbol{x},t), \tag{1}$$

where $p(\boldsymbol{x},t)$ is the pressure difference at a some location $\boldsymbol{x}$ in the liquid at time t, ρ_0 is the rest density taken as constant, and κ is the compressibility of the liquid.

A. Damping Term Derivation

1. *Derivation from Navier Stokes*

Due to the small energy deposition by a single particle in the fluid, it is reasonable to assume that the damping effect caused by the viscosity of the liquid will significantly affect the decay time of the acoustic wave. To derive the viscous wave equation (also known as the strongly damped wave equation [20, 21]) we exploit the principle of conservation of mass Eq. (2) and momentum Eq. (3) and include the damping term $\mu\Delta\boldsymbol{v}$:

$$\frac{\partial\rho}{\partial t} + \boldsymbol{\nabla}\cdot(\rho\boldsymbol{v}) = 0 \tag{2}$$

$$\rho\frac{\partial\boldsymbol{v}}{\partial t} + \rho(\boldsymbol{v}\cdot\boldsymbol{\nabla})\boldsymbol{v} = -\boldsymbol{\nabla}P + \mu\Delta\boldsymbol{v}, \tag{3}$$

where $\rho(\boldsymbol{x},t)$, $P(\boldsymbol{x},t)$, and $\boldsymbol{v}(\boldsymbol{x},t)$ are the density, pressure, and velocity, respectively, while μ is the coefficient of bulk viscosity. As done in in other related literature [19, 21, 22], we assume a fluid with no vorticity ($\boldsymbol{\nabla}\times\boldsymbol{v} = \boldsymbol{0}$). Thus, Navier-Stokes equation Eq. (3) takes the form:

$$\rho\frac{\partial\boldsymbol{v}}{\partial t} + \rho\boldsymbol{v}\cdot\boldsymbol{\nabla}\boldsymbol{v} = -\boldsymbol{\nabla}P + \mu\Delta\boldsymbol{v}. \tag{4}$$

Let us consider a small perturbation to each of the variables:

$$\rho = \rho_0 + \delta\rho \tag{5}$$

$$P = p_0 + \delta p \tag{6}$$

$$\boldsymbol{v} = \boldsymbol{v}_0 + \delta\boldsymbol{v} = \delta\boldsymbol{v}, \tag{7}$$

where ρ_0, p_0, and $\boldsymbol{v}_0$ are the pressure, density, and velocity of the fluid at equilibrium and we have assumed the fluid to be initially at rest. From now on we will exclusively deal with $\delta p, \delta\rho$ and $\delta\boldsymbol{v}$, as such, we will be dropping the delta to keep notation light. By plugging the perturbed variables into Eq. (2) and Eq. (4) and neglecting higher order terms, i.e. $\mathcal{O}((\delta\rho/\rho_0)^2)$, $\mathcal{O}((\delta P/P_0)^2)$, and $\mathcal{O}((\delta v/v_0)^2)$, we obtain the following equations:

$$\frac{\partial\rho}{\partial t} + \rho_0\boldsymbol{\nabla}\cdot\boldsymbol{v} = 0 \tag{8}$$

$$\rho_0\frac{\partial\boldsymbol{v}}{\partial t} + \boldsymbol{\nabla}p = \mu\Delta\boldsymbol{v}. \tag{9}$$

Taking the divergence of Eq. (9) leads to

$$\rho_0\frac{\partial}{\partial t}\boldsymbol{\nabla}\cdot\boldsymbol{v} + \Delta p = \mu\Delta\left(\boldsymbol{\nabla}\cdot\boldsymbol{v}\right), \tag{10}$$

where $\boldsymbol{\nabla}\cdot\boldsymbol{v}$ can be replaced using Eq. (10) to obtain

$$\frac{\partial^2\rho}{\partial t^2} = \Delta\left(p + \frac{\mu}{\rho_0}\frac{\partial\rho}{\partial t}\right) \tag{11}$$

Expressing the density as a function of the compressibility like so: $\rho = \rho_0\kappa p$, Eq. (11) can be expressed only as a function of pressure:

$$\Delta\left(p + \mu\,\kappa\frac{\partial p}{\partial t}\right) = \rho_0\,\kappa\,\frac{\partial^2 p}{\partial t^2} \tag{12}$$

We define the speed of the wave, c, as $c = 1/\sqrt{\rho_0\kappa}$ and the attenuation frequency, ω_0, as $\omega_0 = 1/\mu\kappa$. Thus, Eq. (12) becomes:

$$\Delta\left(p + \frac{1}{\omega_0}\frac{\partial p}{\partial t}\right) = \frac{1}{c^2}\frac{\partial^2 p}{\partial t^2} \tag{13}$$

in a more familiar form.

2. *Damping Characteristic*

We can obtain the dispersion relation of plane wave solutions to Eq. (13) by taking the Fourier transform of the pressure in all components (space and time) as defined later in Eq. (28). Doing so we obtain that the dispersion relation between the frequency ω and wavenumber $k = ||\vec{k}||$ is given by

$$k^2 = \frac{\omega^2}{c^2}\left(1 - i\frac{\omega}{\omega_0}\right)^{-1}. \tag{14}$$

At first glance we notice that this equation at the limit $\omega_0 \to \infty$ which corresponds to the no damping case becomes $kc = \omega$ which is the expected solution.

More importantly however, we can use the relation in Eq.(14) to quickly obtain a hint of how the additional damping term we derived affects the sound wave generated. In particular we see that at low frequency the relation is similar to the undamped case ($\omega \to \infty$). However, as the frequency increases, the wavenumber's imaginary component further increases.

We can deduce the physical significance of the imaginary component of k by plugging it into a plane wave $e^{ik(\omega)r-\omega t}$. Therefore the imaginary part is going to introduce exponential decay in the amplitude of the wave with rate proportional to it. As a result, the imaginary part is the spatial decay rate of the wave and it increases with frequency. In the context of waves generated by particles we observe that the higher frequency components of the generated pressure wave will decay faster and thus the lower frequency components will propagate further. From a detection standpoint we verify that in viscous media it is easier to detect low frequency components as they propagate further.

B. Source Term Derivation

Let us now address the mechanism by which the wave is generated, i.e. the source term in Eq. (1). It is well documented [23, 24] that a particle passing through a liquid deposits energy such that, locally, the temperature sharply increases. The almost instantaneous change in temperature leads to a rapid volume expansion and the subsequent change in density propagates through the liquid. Here, we assume that this effect, referred to as "local heating", is the biggest contributor to the generation of the sound wave. This is consistent with past literature where acoustic signals due to particle beams were studied [5, 19, 25].

1. *Derivation from Navier Stokes*

Let us consider the effect of some local temperature fluctuation $\tau(\boldsymbol{x}, t)$ such that the total temperature is given by $T(\boldsymbol{x}, t) = T_0 + \tau(\boldsymbol{x}, t)$, where T_0 is the equilibrium temperature. With a variation in temperature, density will change as a function of both pressure and temperature. Specifically, at first order (using ρ, p, and τ to denote the changes in density, pressure, and temperature, respectively) we can express the change in density by:

$$\rho = \left.\frac{\partial \rho}{\partial P}\right|_T p + \left.\frac{\partial \rho}{\partial T}\right|_P \tau \tag{15}$$

where P and T represent total pressure and temperature respectively, while V represents a small volume of the liquid around the particle interaction point. Let us recall the definitions of isothermal compressibility κ_T and coefficient of thermal expansion:

$$\kappa_T = -\frac{1}{V}\left.\frac{\partial V}{\partial P}\right|_T = \frac{1}{\rho_0}\left.\frac{\partial \rho}{\partial P}\right|_T \tag{16}$$

$$\beta = \frac{1}{V}\left.\frac{\partial V}{\partial T}\right|_P = -\frac{1}{\rho_0}\left.\frac{\partial \rho}{\partial T}\right|_P. \tag{17}$$

We can then rewrite Eq. (15) as follows:

$$\rho = \rho_0(\kappa_T p - \beta\tau).$$

From here we can proceed just as in Section II A when we derived Eq. (11). First, we use Eq. (15) to write the density in terms of the pressure difference p and temperature fluctuation τ. Then, we assume that, to first order, the functions $\kappa_T(P, T, t)$ and $\beta(P, T, t)$ vary slowly with time, such that:

$$\rho_0\kappa_T\frac{\partial^2 p}{\partial t^2} - \rho_0\beta\frac{\partial^2 \tau}{\partial t^2} = \Delta\left(p + \mu\kappa_T\frac{\partial p}{\partial t} + \mu\beta\frac{\partial \tau}{\partial t}\right). \tag{18}$$

Equation Eq. (18) shows the presence of an extra damping term. However, assuming that the temperature variation is small, $\frac{\partial}{\partial t}\Delta\tau \approx 0$ we may neglect that term. Using the first law of thermodynamics, we can determine the heat per unit volume added to the liquid $\epsilon(\boldsymbol{x}, t)$

$$\epsilon = \frac{\delta Q}{\delta V} = \rho_0 C_p \tau, \tag{19}$$

where C_p is the specific heat capacity of the liquid at constant pressure. We may now introduce the complete wave equation by substituting τ with Eq. (19):

$$\Delta\left(p + \mu\kappa_T\frac{\partial p}{\partial t}\right) - \rho_0\kappa_T\frac{\partial^2 p}{\partial t^2} = -\frac{\beta}{C_p}\frac{\partial^2 \epsilon}{\partial t^2} \tag{20}$$

which may be more compactly written as

$$\Delta\left(p + \frac{1}{\omega_0}p_t\right) - \frac{1}{c^2}p_{tt} = -\frac{\beta}{C_p}\epsilon_{tt}. \tag{21}$$

We have successfully derived the correction terms to the acoustic wave equation Eq. (1) to model the damped wave that is generated by a heat source inside a liquid. In Section IV A, we will show how to estimate the heat deposition $\epsilon(\boldsymbol{x}, t)$ for single, charged particles through liquids using the Bethe-Bloch formula. At this stage it is important to note that our assumption that κ and β do not vary in time is only valid away from the center of heating.

2. *Low Viscosity Assumption*

III. ANALYTIC SOLUTIONS TO THE WAVE EQUATION

In this section we attempt to solve for the acoustic signal due to arbitrary single particles in its general form

using perturbation theory. We first develop a perturbative approximation scheme for the non-homogeneous strongly damped wave equation Eq. (22) based on viscosity. Then we calculate Green's functions for the retarded propagator on each order, and finally, we provide an explicit solution for the first order in viscosity.

In this section we will focus on the following form of Eq. (1) where we have replaced the source term with an arbitrary function $f : \mathbb{R}^4 \to \mathbb{R}$ like so

$$\Box p(\boldsymbol{x}) + \lambda \Delta \partial_t p(\boldsymbol{x}) = -f(\boldsymbol{x}) \tag{22}$$

where λ is the viscosity coefficient p is the pressure, and f is the source function. We note that f is some function with compact support. Later we will impose more restrictions on f to better represent the energy distribution of a moving particle, however, for now we consider a general distribution to come up with Green's Functions for the problem.

A. Approximations Using Perturbation Theory

The solution for the pressure wave p from Eq. (22) is more simply expressed by treating the damping term $\lambda \Delta \partial_t p(\boldsymbol{x})$ as a perturbation for small λ. Specifically we will write the solution as a function of λ like so

$$p(\boldsymbol{x}) = p_0(\boldsymbol{x}) + \lambda p_1(\boldsymbol{x}) + \cdots = \sum_{n=0}^{\infty} \lambda^n p_n(\boldsymbol{x}). \tag{23}$$

Using Eq. (23) we can rewrite the original Equation (22) in terms of the perturbation orders like so

$$\Box p_0(\boldsymbol{x}) + \sum_{n=1}^{\infty} \lambda^n \left[\Box p_n(\boldsymbol{x}) + \Delta \partial_t p_{n-1}(\boldsymbol{x})\right] = -f(\boldsymbol{x}). \tag{24}$$

Therefore for all λ we must have that each order is given by the recursive formula

$$\Box p_0(\boldsymbol{x}) = -f(\boldsymbol{x}) \tag{25}$$
$$\Box p_n(\boldsymbol{x}) = -\Delta \partial_t p_{n-1}(\boldsymbol{x}). \tag{26}$$

Using these expressions we can write an explicit partial differential equation that each term must satisfy

$$\Box^{n+1} p_n(\boldsymbol{x}) = -\left(-\Delta \partial_t\right)^n f(\boldsymbol{x}). \tag{27}$$

Note that for $n = 0$ we have the normal wave equation with source function f. As the order n increases we require that higher orders of the spacetime curvature of the correction to be depended on higher orders of the spatial curvature of the rate at which energy is deposited. In other words, if f is some form of bump function we will end up adding sharper and more oscillatory corrections for each order.

We will now focus on solving the global Cauchy problem for Eq. (27). To do that we will use the method of Green's Functions. Before we do so, however, it is instructive to simplify Eq. (27) using a Fourier transform defined as

$$\hat{f}(\boldsymbol{k}) = \int_{\mathbb{R}^4} d^4x\, f(\boldsymbol{x}) e^{-i\boldsymbol{k}\cdot\boldsymbol{x}} \tag{28}$$
$$f(\boldsymbol{x}) = \int_{\mathbb{R}^4} \frac{d^4k}{(2\pi)^4} \hat{f}(\boldsymbol{k}) e^{i\boldsymbol{k}\cdot\boldsymbol{x}}, \tag{29}$$

where $\boldsymbol{k}\cdot\boldsymbol{x}$ is the four-vector inner product defined by $\boldsymbol{k}\cdot\boldsymbol{x} = k^\alpha x_\alpha = \eta_{\alpha\beta} k_\alpha x_\beta$, where $\eta_{\alpha\beta} = \mathrm{diag}(-1, 1, 1, 1)$ is the Minkowski metric. Using this transformation Eq. (27) transforms to

$$\hat{p}_n(\boldsymbol{k}) = \frac{1}{-\boldsymbol{k}^2} \left(\frac{ik_0\, \vec{k}^2}{-\boldsymbol{k}^2}\right)^n \hat{f}(\boldsymbol{k}), \tag{30}$$

where $\vec{k}^2 = k_1^2 + k_2^2 + k_3^2$ and $\boldsymbol{k}^2 = -k_0^2 + \vec{k}^2$. This is a much simplified formula that completely defines the frequency profile of each term given a source function f. Now we are ready to solve for the Green's Functions.

B. Green's Functions

To provide closed form solutions for arbitrary terms in the perturbative expansion of the pressure Eq. (23) as a function of the viscosity coefficient λ we study a general expression for the retarded propagator of Eq. (27). The reason why we want the retarded propagator is in order to maintain causality for our classical system.

1. *Using Potentials and Residues*

From a calculation perspective however, the form of the propagator simplifies if we solve Eq. (27) not for the n^{th} pressure component p_n in the perturbative expansion, but for a potential ψ_n such that $\partial_t^n \psi_n = p_n$. This way can write Eq. (27) as follows

$$\Box^{n+1} \psi_n(\boldsymbol{x}) = -(-\Delta)^n f(\boldsymbol{x}). \tag{31}$$

To calculate the Green's function $G_n(\boldsymbol{x})$ for order n in the perturbative expansion, we use the Fourier transform defined in (28). By plugging in a δ source, $f(\boldsymbol{x}) = \delta(\boldsymbol{x})$, in Eq. (31) and taking the transformation, we obtain an expression for the fourier transformed Green's function $\hat{G}_n$

$$\hat{G}_n(\boldsymbol{x}) = \frac{1}{-\boldsymbol{k}^2} \left(\frac{\vec{k}^2}{-\boldsymbol{k}^2}\right)^n. \tag{32}$$

Notice the singularities of order $n+1$ at $\boldsymbol{k}^2 = 0$. Particularly they occur when $k_0 = \pm|\vec{k}|$. To extract the retarded propagator in spatial coordinates out of $\hat{G}$ we need to take the inverse Fourier transform defined in Eq. (29)

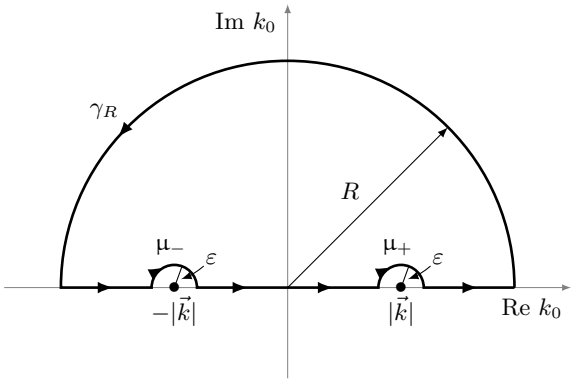

FIG. 1. Integration Contour Γ_ε of k_0 in the inverse Fourier transform of Eq. 32 to obtain the retarded propagator.

with the contour Γ_ε, shown in Fig. 1 as $\varepsilon \to 0$ to preserve causality. Specifically that inverse Fourier transform is given by

$$G_n(\boldsymbol{x}) = \lim_{\varepsilon\to 0} \int_{\Gamma_\varepsilon} \frac{dk_0}{2\pi} e^{-ik_0 t} \int_{\mathbb{R}^3} \frac{d^3k}{(2\pi)^3} \hat{G}_n(\boldsymbol{k})\, e^{i\vec{k}\cdot\vec{x}}. \quad (33)$$

We can rewrite this integral by "nudging" the singularities by ε. To do so we do a coordinate transformation by changing $k_0 \to k_0 + i\varepsilon$ therefore the integral becomes

$$G_n(\boldsymbol{x}) = \lim_{\varepsilon\to 0} \int_{\mathbb{R}^4} \frac{d^4k}{(2\pi)^4} \frac{(\vec{k}^2)^n\, e^{i\boldsymbol{k}\cdot\boldsymbol{x}}}{\left[(k_0+i\varepsilon)^2 - \vec{k}^2\right]^{n+1}}. \quad (34)$$

We can now do the k_0 integral first using residue theorem. Note that in this form the singularities are at $k_0 = \pm|\vec{k}| - i\varepsilon$. Their analytic form of the residues is quite involved, therefore before we calculate them we will extract some of their properties as follows.

2. Properties of Residues

We notice that both of the singularities are on the lower half of the complex plane. Therefore, for $t < 0$ where the integral converges at the upper half plane (as shown in Fig. 1) the contour encloses no singularities, therefore the integral is 0. For $t > 0$ the contour includes the singularities.

Let's denote the two residues by $\hat{g}_\pm(\vec{k}^2)$ corresponding to the singularities at $\pm|\vec{k}| + i\varepsilon$ respectively. Clearly they are functions of $\vec{k}^2$ as well as n and ε. By using the residue theorem around a small enough circle that contains only one of the singularities, we can prove that the residues are related according to

$$\hat{g}_+(\vec{k}^2) = -\hat{g}_-^*(\vec{k}^2), \quad (35)$$

where the * denotes the complex conjugate. This is a really convenient way of writing as we can rewrite the integral in Eq. (34) using the residue theorem like so

$$G_n(\boldsymbol{x}) = \Theta(t) \lim_{\varepsilon\to 0} \int_{\mathbb{R}^3} \frac{d^3k}{(2\pi)^3} \hat{g}_n(\vec{k}^2) e^{i\vec{k}\cdot\vec{x}}, \quad (36)$$

where $\Theta(t)$ is the Heaviside function, and we have denoted by $\hat{g}_n(\vec{k}^2)$ the sum of the residues given by

$$\hat{g}_n(\vec{k}^2) = i\hat{g}_+(\vec{k}^2) - i\hat{g}_+^*(\vec{k}^2) = -2\mathrm{Im}\hat{g}_+(\vec{k}^2), \quad (37)$$

where the last step is carried out using (35). This way, not only we managed to, somewhat, simplify the transform, but we have also shown that the Green's function is real for all orders n. That is because $\hat{g}_n$ is radially symmetric in k and real valued (since it is the imaginary part of a complex valued function), hence the inverse Fourier transform must be real.

3. Calculation of Residues and Green's Functions

We are now ready to calculate the analytic expression of the residues at the two singulaties where $k_0 = k_\pm = \pm|\vec{k}| + i\varepsilon$. From what we have shown above, it is enough to calculate the residue at $k_0 = k_+$. We do so using the Laurent expansion of the integrand in Eq. (34). By calculating a series representation centered at $k_0 = k_+$ for each term of the equation, and then multiplying them together, we obtain that the coefficient of the $(k_0 - k_+)$ term is given by

$$\begin{aligned}\hat{g}_+ &= \lim_{\varepsilon\to 0} -e^{-\varepsilon t}\Theta(t)\,\mathrm{Im}\,\frac{e^{i(\vec{k}\cdot\vec{x}-|\vec{k}|t)}}{2^n|\vec{k}|}P(|\vec{k}|) \\ &= -\Theta(t)\,\frac{\sin(\vec{k}\cdot x - |\vec{k}|t)}{2^n|\vec{k}|}P(|\vec{k}|),\end{aligned} \quad (38)$$

where $P(k)$ denotes a polynomial of $|\vec{k}|$ given by

$$P(|\vec{k}|) = (-1)^n \sum_{m=0}^{n} \frac{(2i|\vec{k}|t)^m}{m!}\binom{2n-m}{n}. \quad (39)$$

Expressing the residue we can now plug it into the integral using spherical coordinates to obtain the final expression of the Green's function G_n for the potential ψ_n as

$$\begin{aligned}G_n(\boldsymbol{x}) = \frac{\Theta(t)}{4^{n+1}\pi r} \sum_{m=0}^{n} \frac{(-2t)^m}{m!}\binom{2n-m}{n} \\ \left[\delta^{(m)}(t-r) - \delta^{(m)}(t+r)\right],\end{aligned} \quad (40)$$

where $r = |\vec{x}|$. Using $\Theta(t)$ we can simplify the expression above and by grouping the constants we get

$$G_n(\boldsymbol{x}) = \sum_{m=0}^{n} \frac{(-2)^m}{4^{n+1}\pi m!}\binom{2n-m}{n} G_{nm}(\boldsymbol{x}), \quad (41)$$

where $G_{nm}(\boldsymbol{x})$ is given by

$$G_{nm}(\boldsymbol{x}) = \frac{t^m}{r}\delta^{(m)}(t-r). \tag{42}$$

Note that we manage to express G_{nm} like so by using the fact that $\Theta(t)\delta(r+t) = 0\ \forall r > 0$. Therefore we can use the above green's functions to calculate the pressure for any arbitrary source function f like so

$$p(\boldsymbol{x}) = \sum_{n=0}^{\infty} \partial_t^n \left(G_n * f\right)(\boldsymbol{x}). \tag{43}$$

C. Causality

A quick obsevation from form the expression of the Green's functions for each order (Eq. (41)) is that we can factor out a Heaviside theta. This way we can show that our propagator is indeed causal (as in the future is affected only by the past) since when we convolve Eq. (41) with the source function f to obtain the solution we end up with the following integral because of the Heaviside in G_n

$$p_n(\boldsymbol{x}) = \int_{-\infty}^{t} dt' \int_{\mathbb{R}^3} d^3x'\, G_n(\boldsymbol{x}-\boldsymbol{x}')f(\boldsymbol{x}'). \tag{44}$$

Therefore, we can see that each perturbation order in pressure p_n depends on the shape of the source before time t.

D. Closed Form solution for Delta Source

With an analytic expression for the n^{th} order, calculated in Eq. (41), we can now provide an solution for a delta source function for f in closed form. In particular, we want to distribute the energy density over space using a moving delta function of the form $\delta(x)\delta(y)\delta(z-vt)$ where v is the speed of the particle in the units where the speed of sound $c = 1$. Assuming that the energy density that the particle deposits as a function of time is given by a function $q(t)$ we can proceed by defining f by

$$f(\boldsymbol{x}) = q(t)\delta(x)\delta(y)\delta(z-vt). \tag{45}$$

Using Eq. (44) we see need to calculate the convolutions $(G_n * f)(\boldsymbol{x})$. Since convlution is a linear operation we can calculate this by calculating the convolution for each component G_{nm} in the expansion shown in Eq. (41). Then each term of the convolution can be computed by

$$G_{nm} * f(\boldsymbol{x}) = \int_{\mathbb{R}^3} d^3x' \int_{\mathbb{R}} dt'\, G_{nm}(\boldsymbol{x}')f(\boldsymbol{x}-\boldsymbol{x}'), \tag{46}$$

where the primed variables in $\boldsymbol{x}'$ are the convolution variables. Plugging the functions in and calculating we obtain the following expression:

$$G_{nm} * f(\boldsymbol{x}) = \sum_{l=0}^{m}\sum_{z'_k\in S} (-1)^l l! \binom{m}{l}^2 v^{m-l} \partial_{z'}^{m-l}\left[\frac{q(t-r)r^{m-l}}{r-vz'}\right](z'_k), \tag{47}$$

where v is the speed of the particle, $r = \sqrt{x^2+y^2+z'^2}$, and S is the set of solutions z'_k of the equation

$$z' - (z-vt) = vr(z'), \tag{48}$$

where, again, $r(z')$ is the radius as a function of z' given by $r(z') = \sqrt{x^2+y^2+z'^2}$. While this looks somewhat involved, we can use it to more compactly write the convolution $\psi_n = G_n * f$ like so

$$\psi_n(\boldsymbol{x}) = \sum_{m,l}^{n,m}\sum_{z'_k\in S} C_{nml}\,\partial_{z'}^{m-l}\left[\frac{q(t-r)(vr)^{m-l}}{r-vz'}\right](z'_k), \tag{49}$$

where C_{nml} is a constant multiplier given by

$$C_{nml} := \frac{(-1)^{l+m}\,2^m l!}{4^{n+1}\pi m!}\binom{2n-m}{n}\binom{m}{l}^2. \tag{50}$$

This expression shows that the potential is given by derivatives of the same function, evaluated at the roots of Eq. (48). The physical meaning of the roots as well as their analytic form is shown in the next section.

E. Sound sources for different particle speeds

In Eq. (49) we have shown that the derivative is evaluated at certain "special" points that are the roots of Eq. (48). Solving this equation we obtain the following two solutions

$$z'_{\pm} = \gamma^2(z-vt) \pm |v|\sqrt{\gamma^4(z-vt)^2 + \gamma^2\rho^2}, \tag{51}$$

where $\gamma^2 = 1/(1-v^2)$, and $\rho = \sqrt{x^2+y^2}$ is the distance perpendicular to the path of the particle. However, as is obvious from Eq. (48) and the inside of the square root in Eq. (51), these solutions do not always apply. To explore the physical meaning behind which solutions are kept under what conditions we turn back to the integral representation of the convolution with the source function in Eq. (46).

Ordinarily we would think of the wave generated by a moving particle as the sum of the sound waves generated by each point along it's motion. The form of those sound waves is given by the retarded propagator we have calculated in Eq. (41). Therefore, when an observer at spacetime point $\boldsymbol{x}$ observes a sound wave, we can trace it back to a point in the particle's track where it was generated.

An equivalent way of thinking about this is instead of shooting waves along the path of the particle to shoot particles along the path of a wave. This is the approach we have implemented in the integral in Eq. (46). The equivalence is made rigorous by the commutativity of the convolution. Therefore Eq. (48), in fact, predicts the points of intersection between a virtual particle passing through an observer located at $\boldsymbol{x}$ and a prototype wave from the origin (described by the propagator). This is shown clearly in Fig. 2.

1. *Slow Particles*

To find out which solutions from $z'_\pm$ shown in Eq. (51) are applicable when the speed of the particle is less than the speed of sound $v < 1$ we notice the following. Initially, $v < 1 \implies \gamma^2 > 0$, hence $z'_\pm$ is defined for all values of z, t, and r. Therefore, the only condition left comes from Eq. (48) that we can restate as

$$z' - (z - vt) > 0. \tag{52}$$

Using this condition the only solution that satisfies Eq. (48) is z'_+. Therefore for $v < 1$ $S = \{z'_+\}$, which is also schematically shown in Fig. 2.

2. *Fast Particles*

In the case of particles moving faster than the speed of sound ($v > 1$) the considerations become more niche. Fig. 3 illustrates that there are some events with positive time that the signal will never reach. Mathematically this is when the square root of $z'_\pm$ in Eq. (51) becomes imaginary. This is possible since $v > 1 \implies \gamma^2 < 0$. In such case, the delta function in the convolution will have no zeros hence the signal would be zero. This happens when

$$vt < z + \rho\sqrt{v^2 - 1}. \tag{53}$$

When the condition in Eq. (53) is satisfied we can show that Eq. (52) implies that for $(z - vt) > 0$ no solution exists, hence the pressure generated there is 0. However, when $(z - vt) < 0$ both solutions $z'_\pm$ hold hence $S = \{z'_+, z'_-\}$.

F. Leading Order Analytic Solution

To make our model a little less abstract we will explicitly provide a closed form solution for $n = 0$ i.e. the undamped wave equation. The propagator is given by plugging $n = 0$ to Eq. (49) and obtaining

$$p(\boldsymbol{x}) = \sum_{z'_k \in S} \partial_t \frac{q(t - r(z'_k))}{4\pi\,(r(z'_k) - vz'_k)} \tag{54}$$

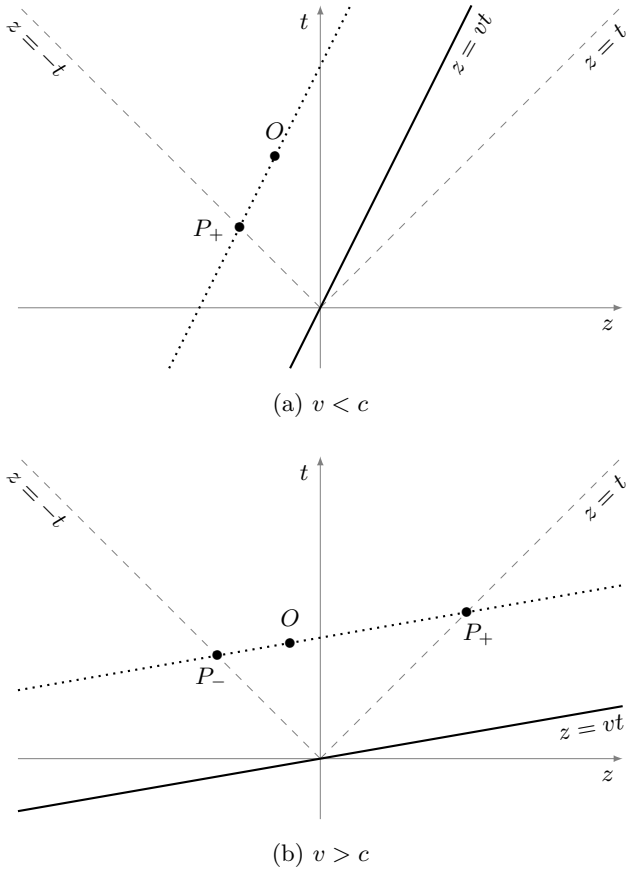

FIG. 2. Minkowski diagrams for sources moving slower (a) or faster (b) than the speed of sound $c = 1$ on the medium. We can see that for slow particles (a) an observer O observes the sound emitted from P_+. However, when the source moves faster than the speed of sound (b) the observer at O observes the sound emitted from both P_- and P_+. In Eq. (48) we solve for the z-coordinate of these points.

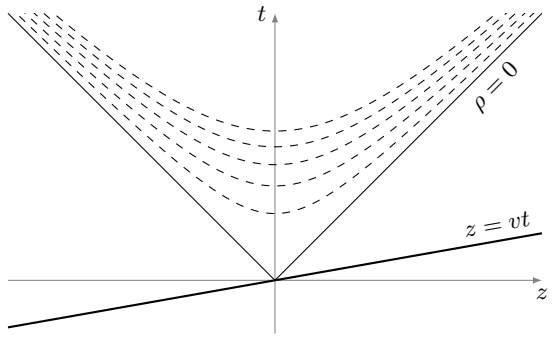

FIG. 3. The prototype generated wave on the $z - t$ plane as a family of curves for progressively larger perpendicular radii ρ starting from 0. We can see that if $v > 1$, there are observers between the solid and dashed lines that for larger values of ρ will have no intersection with the particle path.

where the set of solutions S is defined above for different values of v and $\boldsymbol{x}$. Assuming that the particle immediately starts depositing energy at time $t = 0$ we can set $q(t) = \Theta(t)$ the Heaviside function. Using a heaviside our solutions from Eq. (54) simplify further to

$$p(\boldsymbol{x}) = -\frac{v\bar{z}\,\Theta(-\bar{z} - \rho\sqrt{v^2-1})}{[\bar{z}^2 + \rho^2(1-v^2)]^{\frac{3}{2}}}, \tag{55}$$

where $\bar{z} = z - vt$, Θ is the Heaviside theta function, and $r = \sqrt{x^2+y^2+z^2}$ the radius of the observer from the point where the energy deposition starts. We notice that the supersonic particles ($v > 1$) produce different signals than subsonic ($v < 1$). This is a well known result from the wave equation, however as the dominant term for the low viscosity case, we can use the classical wave equation solution (term for $n = 0$) to predict the point and time when a maximum signal occurs as a function of the perpendicular distance from the particle track ρ. For the subsonic case we note that this is at the point when the derivative of the multi-variable function vanishes in all of it's components. This condition is given by

$$(z - vt)^2 = \frac{\rho^2}{2\gamma^2}. \tag{56}$$

For supersonic particles we notice that even away from $\rho = 0$ we have a singularity in the pressure at the zeroth order. This singularity is located at a shell in $\mathbb{R}^3$ defined by $\rho^2 + z^2 = t^2$. Using that representation, given a value of ρ we obtain the maximum will be located at

$$\begin{aligned} z^2 &= -\rho^2\gamma^2 \\ t &= r, \end{aligned} \tag{57}$$

where we should note that in the supersonic case $v > 1 \implies \gamma^2 < 0$. We use these results in the next section to examine the pressure around those special points to obtain an estimate of the signal created by the particles.

IV. APPLICATIONS TO MIPS

Having a perturbative expansion that works for different type of source terms we can use it to predict the acoustic signal produced by single particles. In this section we provide a calculation of the acoustic signal generated by muons as a model for a Minimum Ionizing Particle. To do so, we derive an expression of the distribution of the rate of energy deposition of the particle and use it as a source term for the model derived in III. Then we simulate the evolution of the sound waves to predict peak pressures at various particle speeds in different materials.

A. Energy Deposition Estimation

To model the effect of a particle going through a fluid, we will ignore any nonlinear effects, such as direct collisions between the particle and the fluid molecules. That way we will be able to analytically describe the average energy deposition of the particle. Multiple attempts to describe the energy deposition profile of a single charged particles can be found in literature [19, 26]. For the purposes of our analysis we are using the Bethe-Bloch formula [42] to obtain an accurate estimate of the energy lost by the particle in the medium. However, according to Amsler et. al. [43] we recognize that the average $\langle dE/dx\rangle$ is not a correct estimate of the energy deposited for a single particle due to the skewness of the distribution. Hence why the most probable value from the Bethe distribution is used in our calculations and is described by [23]

$$\left.\frac{dE}{dx}\right|_M = \xi\left[\ln\frac{2m_e c_l^2\beta^2\gamma^2}{I} + \ln\frac{\xi}{I} - \beta^2\right], \tag{58}$$

where ξ is a characteristic energy given in [23], I is the mean excitation energy of liquid, m_e the mass of an electron, only in this fomrula we have that c_l is the speed of light (and not sound) along with γ the Lorenz factor and $\beta = v/c_l$ the speed of the particle relative to the speed of light. The primary assumptions we made were that the particles travel at a straight line through the fluid (along $\hat{\boldsymbol{x}}$) and that they have high enough energy that the deposition in the medium does not change their speed appreciably. In more rigorous terms we assume that

$$\frac{d}{dt}\frac{dE}{dx} = 0. \tag{59}$$

As a result, the rate at which energy is deposited in the medium can be given by

$$\frac{dE}{dt} = \frac{dx}{dt}\left.\frac{dE}{dx}\right|_M = v\left.\frac{dE}{dx}\right|_M, \tag{60}$$

where v is the speed of the particle through the fluid. Furthermore we can set up a cylindrical coordinate system around $\hat{\boldsymbol{x}}$ where the particle would always be at position $(\rho, \phi, x) = (0, 0, vt)$ at time t. As a result, what we now need to derive, is the rate of change energy density $\epsilon_t(\boldsymbol{x}, t) = \epsilon_t(\rho, x, t) = dE/dt\, d\Omega$ in order to plug in to the wave equation (21).

To do so, consider the energy deposition in some volume Ω. The rate of energy deposition over the volume can be written as (using (60))

$$\frac{dE}{dt} = \int_\Omega d\Omega\, v\left.\frac{dE}{dx}\right|_M G(\boldsymbol{x}), \tag{61}$$

where $G(\boldsymbol{x})$ is the spatial distribution of the energy deposited by the particle. From (61) we can derive that the rate of change of energy density, in cylindrical coordinates, can be given by

$$\epsilon_t(\boldsymbol{x}, t) = \epsilon_t(\rho, \phi, x, t) = \frac{dE}{dt}G(\rho, \phi, x - vt). \tag{62}$$

TABLE I. constants relevant to the calculation for acoustic signals in various fluids. The constants were found in references [27–41]

Name	Temperature[a] $T\ (K)$	Density $\rho_0\ (kg\,m^{-3})$	Sound Speed $c\ (m\,s^{-1})$	Viscosity $\mu\ (\times 10^4\ Pa\,s)$	Source Term Multiplier $\frac{\beta}{C_p}\ (\times 10^6\,kg\,J^{-1})$	Mean Excitation Energy[b] $I\ (eV)$
Water	298.15	997.02	1496.60	8.90030	0.06122	79.70
Nitrogen	77.00	807.20	853.50	1.61980	2.72482	82.00
Argon	84.00	1415.67	861.24	2.88490	3.98389	188.00
Xenon	165.00	2942.40	643.27	5.10420	6.66136	482.00
Mercury	298.15	13600.00	1450.10	16.85000	1.27989	799.97

[a] All pressures are at $P = 1$ atm
[b] The scalar multiplier in front of the source term in Eq. (21)

At this point, inspired by [19, 23], we choose a delta distribution for G. Since our distribution is cylindrically symmetric we can express ϵ_t as

$$\epsilon_t(\rho, x, t) = v \left.\frac{dE}{dx}\right|_M \delta^2(\rho)\delta(x - vt), \tag{63}$$

where ρ is the perpendicular distance from the particle track, v the speed of the particle, and x the distance along the track.

The last addition we need for the rate of energy density deposition in the fluid is an activation term $q(t)$. This is a function $q : \mathbb{R} \to [0, 1]$ that only depends on the time and it is meant to describe when in time is the source "turned on," as in when does the particle starts depositing energy in the liquid detector. In Section III F where we calculated the leading order analytically, we used a Heaviside step function for q, however the discontinuity of the Heaviside leads to a singularity in the pressure that is non physical. A better model for this turning on function q is a sigmoid function

$$q(t) = \frac{1}{1 + e^{-\alpha t}}, \tag{64}$$

where α is a free parameter that dictates the gradient of the transition as shown in Fig. 4. This is a free parameter in this model whose value would affect the peak pressure of the signal, and should be adjusted based on the application.

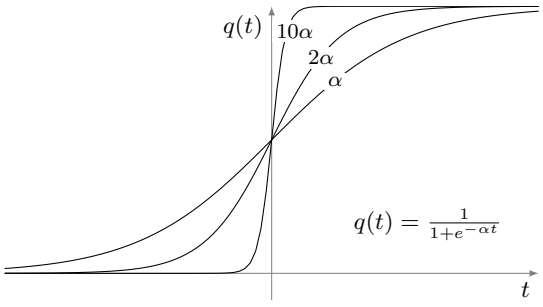

FIG. 4. Activation function for the source term in Eq. (65) as a function of parameter α. The higher α the more $q(t)$ tends to a Heaviside step.

As a result the full source term is given by

$$\epsilon_t(\rho, x, t) = v \left.\frac{dE}{dx}\right|_M q(t)\delta^2(\rho)\delta(x - vt), \tag{65}$$

where $q(t)$ is the activation function described in the previous paragraph, $\left.\frac{dE}{dx}\right|_M$ is the rate of energy deposition by the particle in the liquid, and v is the speed of the particle. Notice that the source term in Eq. 65 is similar to the model source term in Eq. 45 simply multiplied by a constant. We will use this in the following section to calculate the acoustic signals of muons in multiple materials.

B. Numerical Estimates for Muon Signal in Different Media

In this section we apply the model developed to calculate the acoustic signals of relativistic muons passing through water, liquid argon, liquid xenon, liquid nitrogen, and mercury.

To make the calculation of the acoustic signals of single charged particles through different fluids we created a python package that symbolically evaluates any number of terms from Eq. (49) in parallel, and then uses the computer's graphics card to calculate the pressure. The code, installation instructions, and tutorials are found in [44].

We collected constants relevant to the calculation of acoustic signals through various fluids in Table I. Using our simulation and the constants in Table I we were able to calculate quantitative characteristics for the passage of relativistic muons ($\beta = 0.9$) through these fluids.

Specifically, Fig. 5 shows the maximum pressure observed p_m at $\rho = 1cm$ away from the particle track as a function of time. As it is evident, the particles generate a skewed pulse over time that peaks at the scale of fempto Pascal ($10^5\ Pa$). Materials with a higher density and coefficient of thermal expansion like mercury would seem as ideal fluids to maximize the signal under the same particle. Table II contains an accurate numerical estimate of

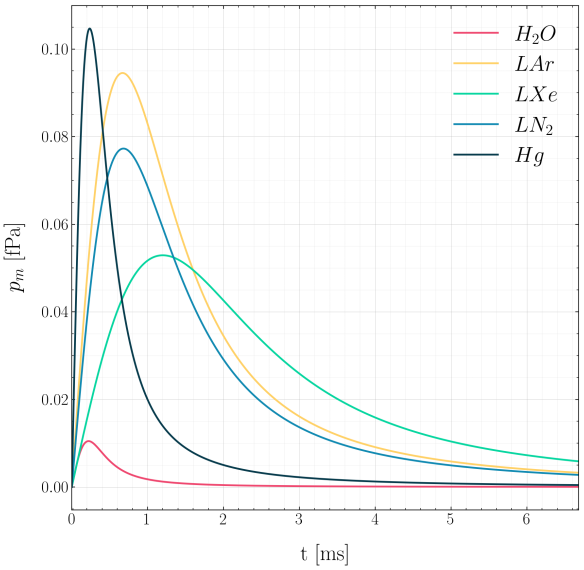

FIG. 5. Peak pressure p_m as a function of time t at distance $\rho = 1$ cm in various liquids of the acoustic signal produced by relativistic muons ($\beta = 0.9$). Denser liquids with large coefficient of thermal expansion seem to produce higher peaks for the same particles.

TABLE II. Peak pressure p_m of the acoustic signal produced by a single relativistic muon $\beta = 0.9$ in various liquids. The parameters were calculated using the simulation in [44] and the constants in Table I.

Name	Temperature[a] $T\ (K)$	Peak Pressure $p_m\ (\times 10^7\ Pa)$
Water	298.15	1.0499
Nitrogen	77.00	7.7324
Argon	84.00	9.4589
Xenon	165.00	5.2946
Mercury	298.15	10.4703

[a] All pressures are at $P = 1$ atm

the peak pressure achieved at a distance $\rho = 1cm$ from the track of the muon.

The dependence of the peak pressure on the radius of the particle is shown in Fig. 6a. In this figure, there is a strong exponential trend after $10^{-1}\,m$ while a peak seems to have been reached before that. Finally this trend continues to appear with an exponential decay of the peak pressure signal as a function of velocity of the incoming muons β as seen in Fig. 6b.

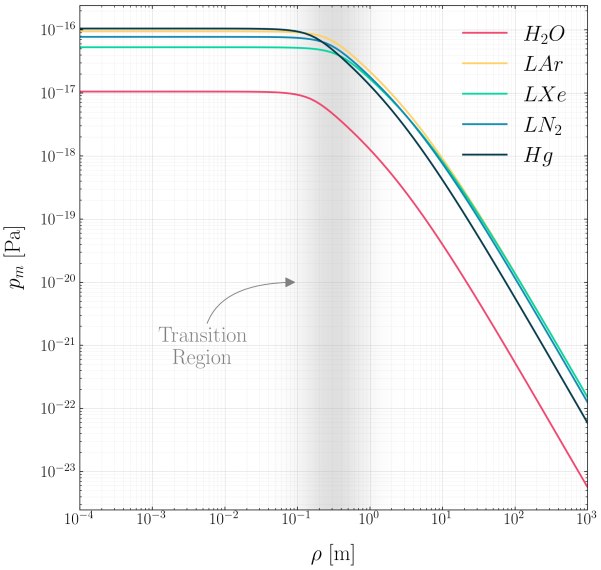

(a) Pressure VS Distance

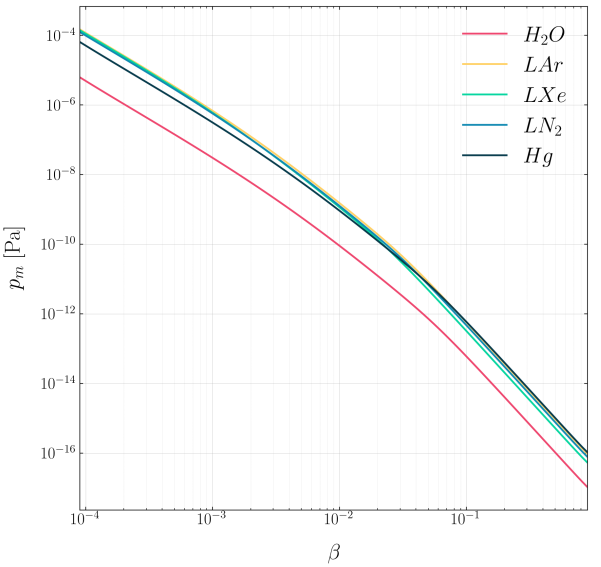

(b) Pressure VS Speed

FIG. 6. Peak pressure p_m of the acoustic signal produced by muons in various liquids. Subfigure 6a presents the peak pressure as a function of distance from the particle track ρ of the acoustic signal produced by relativistic muons ($\beta = 0.9$). Subfigure 6b presents the peak pressure as a function of the muon's fractional lightspeed $\beta = v/c_l$.

V. CONCLUSION

We have presented a complete methodology for calculating the acoustic signals from particle-like energy depositions in liquids with small, but non-negligible viscosity. Furthermore, we have applied our model to predict the signal from relativistic muons crossing multiple liquids. In this analysis we have only considered thermal produc-

tion of sound

The simulation and python package created [44] can be easily incorporated in simulations to predict the signal generated by multiple particle types in different media. All the assumptions of the model are clearly listed in the derivations provided in the earlier sections, along with a complete description of the physical phenomena at play.

Analytically calculating leading and second order corrections due to viscosity, we can extend the observation made by Learned in [19] to the signals produced by single particles in small viscous liquids. Namely that such acoustic signals decay in a power law with distance instead of an exponential one, making their detection not entirely impossible. However, the signal we predict is of very low frequency and peak amplitude, something consistent with the much lower energy deposition of single particles.

Currently, further study is undertaken to completely characterize the effect of viscosity non-perturbatively in order to extend our findings to highly viscous fluids. Another direction we are currently exploring due to the small energies and signals involved is the creation of an Effective Field Theory for this effect, with the promise of simplifying calculation and accounting for quantum effects. In the experimental side, we acknowledge that this level of signal is too small to be detected with traditional methods such as hydrophones, or sparsely places squids. Nevertheless, it is worth pursuing other means of detection such as dense sheets of capacitors, etc. (Find more applications)

[1] G. A. Askaryan, The Soviet Journal of Atomic Energy **3**, 921 (1957).

[2] R. Lahmann, G. Anton, K. Graf, J. Hößl, A. Kappes, U. Katz, K. Mecke, and S. Schwemmer, Astroparticle Physics **65**, 69 (2015).

[3] A. Roberts, Rev. Mod. Phys. **64**, 259 (1992).

[4] A. Karle, J. Ahrens, J. Bahcall, X. Bai, T. Becka, K.-H. Becker, D. Besson, D. Berley, E. Bernardini, D. Bertrand, F. Binon, A. Biron, S. Böser, C. Bohm, O. Botner, O. Bouhali, T. Burgess, T. Castermans, D. Chirkin, J. Conrad, J. Cooley, D. Cowen, A. Davour, C. De Clercq, T. DeYoung, P. Desiati, J.-P. Dewulf, B. Dingus, R. Ellsworth, P. Evenson, A. Fazely, T. Feser, T. Gaisser, J. Gallagher, R. Ganugapati, A. Goldschmidt, J. Goodman, A. Hallgren, F. Halzen, K. Hanson, R. Hardtke, T. Hauschildt, M. Hellwig, P. Herquet, G. Hill, P. Hulth, K. Hultgvist, S. Hundertmark, J. Jacobsen, G. Japaridze, A. Karle, L. Köpke, M. Kowalski, J. Lamoureux, H. Leich, M. Leuthold, P. Lindahl, I. Liubarsky, J. Madson, P. Marciniewski, H. Matis, C. McParland, Y. Minaeva, P. Miočinović, R. Morse, R. Nahnhauer, T. Neunhöffer, P. Niessen, D. Nygren, H. Ogelman, P. Olbrechts, C. Pérez de los Heros, A. Pohl, P. Price, G. Przybylski, K. Rawlins, E. Resconi, W. Rhode, M. Ribordy, S. Richter, H.-G. Sander, T. Schmidt, D. Schneider, D. Seckel, M. Solarz, L. Sparke, G. Spiczak, C. Spiering, T. Stanev, D. Steele, P. Steffen, R. Stokstad, P. Sudhoff, K.-H. Sulanke, G. Sullivan, T. Sumners, I. Taboada, L. Thollander, S. Tilav, C. Walck, C. Weinheimer, C. Wiebusch, C. Wiedemann, R. Wischnewski, H. Wissing, K. Woschnagg, and S. Yoshida, Nuclear Physics B - Proceedings Supplements **118**, 388 (2003), proceedings of the XXth International Conference on Neutrino Physics and Astrophysics.

[5] G. Askaryan, B. Dolgoshein, A. Kalinovsky, and N. Mokhov, Nuclear Instruments and Methods **164**, 267 (1979).

[6] L. Sulak, T. Armstrong, H. Baranger, M. Bregman, M. Levi, D. Mael, J. Strait, T. Bowen, A. Pifer, P. Polakos, H. Bradner, A. Parvulescu, W. Jones, and J. Learned, Nuclear Instruments and Methods **161**, 203 (1979).

[7] Y. L. Jiang, Y. K. Yuan, Y. G. Li, D. B. Chen, R. T. Zheng, J. N. Song, and Y. L. Jiang, in *19th International Cosmic Ray Conference (ICRC19), Volume 8*, International Cosmic Ray Conference, Vol. 8 (1985) p. 329.

[8] T. Bowen, in *International Cosmic Ray Conference*, International Cosmic Ray Conference, Vol. 11 (1979) p. 184.

[9] V. Albul, V. Bychkov, K. Gusev, V. Demidov, E. Demidova, S. Konovalov, A. Kurchanov, V. Luk'yashin, V. Lyashuk, E. Novikov, A. Rostovtsev, A. Sokolov, U. Feizkhanov, and N. Khaldeeva, Instruments and Experimental Techniques **44**, 327 – 334 (2001).

[10] Budnev, N.M., Avrorin, A.D., Avrorin, A.V., Aynutdinov, V.M., Bannasch, R., Belolaptikov, I.A., Bogorodsky, D.Yu., Brudanin, V.B., Danilchenko, I.A., Domogatsky, G.V., Doroshenko, A.A., Dyachok, A.N., Dzhilkibaev, Zh.-A.M., Fialkovsky, S.V., Gafarov, A.R., Gaponenko, O.N., Golubkov, K.V., Gress, T.I., Honz, Z., Kebkal, K.G., Kebkal, O.G., Konischev, K.V., Korobchenko, A.V., Koshechkin, A.P., Koshel, F.K., Kozhin, A.V., Kulepov, V.F., Kuleshov, D.A., Ljashuk, V.I., Milenin, M.B., Mirgazov, R.R., Osipova, E.R., Panfilov, A.I, Pankov, L.V., Perevalov, A.A., Pliskovsky, E.N., Rjabov, E.V, Rozanov, M.I., Rubtzov, V.Yu., Shaybonov, B.A, Sheifler, A.A., Shelepov, M.D, Shkurihin, A.V., Smagina, A.A., Suvorova, O.V., Tabolenko, V.A, Tarashansky, B.A., Yakovlev, S.A., Zagorodnikov, A.V, and Zurbanov, V.L., EPJ Web Conf. **135**, 06004 (2017).

[11] A. Ishihara (IceCube), PoS **ICRC2019**, 1031 (2021), arXiv:1908.09441 [astro-ph.HE].

[12] N. Nosengo, Nature **462**, 560 (2009).

[13] D. Baxter, C. J. Chen, M. Crisler, T. Cwiok, C. E. Dahl, A. Grimsted, J. Gupta, M. Jin, R. Puig, D. Temples, and J. Zhang, Phys. Rev. Lett. **118**, 231301 (2017).

[14] M. Barnabé-Heider, M. Di Marco, P. Doane, M.-H. Genest, R. Gornea, R. Guénette, C. Leroy, L. Lessard, J.-P. Martin, U. Wichoski, V. Zacek, K. Clark, C. Krauss, A. Noble, E. Behnke, W. Feighery, I. Levine, C. Muthusi, S. Kanagalingam, and R. Noulty, Nuclear Instruments and Methods in Physics Research Section A: Accelerators, Spectrometers, Detectors and Associated Equipment **555**, 184 (2005).

[15] E. Behnke, J. I. Collar, P. S. Cooper, K. Crum, M. Crisler, M. Hu, I. Levine, D. Nakazawa,

H. Nguyen, B. Odom, E. Ramberg, J. Rasmussen, N. Riley, A. Sonnenschein, M. Szydagis, and R. Tschirhart, Science **319**, 933 (2008), https://www.science.org/doi/pdf/10.1126/science.1149999.

[16] C. Amole, M. Ardid, I. J. Arnquist, D. M. Asner, D. Baxter, E. Behnke, M. Bressler, B. Broerman, G. Cao, C. J. Chen, U. Chowdhury, K. Clark, J. I. Collar, P. S. Cooper, C. B. Coutu, C. Cowles, M. Crisler, G. Crowder, N. A. Cruz-Venegas, C. E. Dahl, M. Das, S. Fallows, J. Farine, I. Felis, R. Filgas, F. Girard, G. Giroux, J. Hall, C. Hardy, O. Harris, T. Hillier, E. W. Hoppe, C. M. Jackson, M. Jin, L. Klopfenstein, T. Kozynets, C. B. Krauss, M. Laurin, I. Lawson, A. Leblanc, I. Levine, C. Licciardi, W. H. Lippincott, B. Loer, F. Mamedov, P. Mitra, C. Moore, T. Nania, R. Neilson, A. J. Noble, P. Oedekerk, A. Ortega, M.-C. Piro, A. Plante, R. Podviyanuk, S. Priya, A. E. Robinson, S. Sahoo, O. Scallon, S. Seth, A. Sonnenschein, N. Starinski, I. Štekl, T. Sullivan, F. Tardif, E. Vázquez-Jáuregui, N. Walkowski, E. Weima, U. Wichoski, K. Wierman, Y. Yan, V. Zacek, and J. Zhang (PICO Collaboration), Phys. Rev. D **100**, 022001 (2019).

[17] Amole, C., Ardid, M., Asner, D. M., Baxter, D., Behnke, E., Bhattacharjee, P., Borsodi, H., Bou-Cabo, M., Brice, S. J., Broemmelsiek, D., Clark, K., Collar, J. I., Cooper, P. S., Crisler, M., Dahl, C. E., Das, M., Debris, F., Dhungana, N., Farine, J., Felis, I., Filgas, R., Fines-Neuschild, M., Girard, F., Giroux, G., Hai, M., Hall, J., Harris, O., Jackson, C. M., Jin, M., Krauss, C., Lafrenière, M., Laurin, M., Lawson, I., Levine, I., Lippincott, W. H., Mann, E., Martin, J. P., Maurya, D., Mitra, P., Neilson, R., Noble, A. J., Plante, A., Podviyanuk, R., Priya, S., Robinson, A. E., Ruschman, M., Scallon, O., Seth, S., Sonnenschein, A., Starinski, N., Stekl, I., Vázquez-Jáuregui, E., Wells, J., Wichoski, U., Zacek, V., and Zhang, J., EPJ Web of Conferences **95**, 04020 (2015).

[18] S. D. Hunter, LSU Historical Dissertation and Theses 10.31390/gradschool_disstheses.3639 (1981).

[19] J. G. Learned, Physical Review D **19**, 3293 (1979).

[20] M. C. Bortolan and A. N. Carvalho, Topological Methods in Nonlinear Analysis **46**, 563 (2015).

[21] E. M. Viggen, Philosophical Transactions of the Royal Society A: Mathematical, Physical and Engineering Sciences **369**, 2246 (2011).

[22] M. Settnes and H. Bruus, Phys. Rev. E **85**, 016327 (2012).

[23] D. Groom and S. Klein, Passage of particles through matter, in *Review of Particle Physics 2021*, Vol. 2021 (Particle Data Group, 2021) pp. 389 – 412.

[24] G. J. Kutcher and A. E. S. Green, Radiation Research **67**, 408 (1976).

[25] J. Vandenbroucke, G. Gratta, and N. Lehtinen, The Astrophysical Journal **621**, 301–312 (2005).

[26] R. Lahmann, Nuclear and Particle Physics Proceedings **273-275**, 406 (2016).

[27] M. L. Huber, R. A. Perkins, A. Laesecke, D. G. Friend, J. V. Sengers, M. J. Assael, I. N. Metaxa, E. Vogel, R. Mareš, and K. Miyagawa, Journal of Physical and Chemical Reference Data **38**, 101 (2009), https://doi.org/10.1063/1.3088050.

[28] W. Wagner and A. Pruß, Journal of Physical and Chemical Reference Data **31**, 387 (2002), https://doi.org/10.1063/1.1461829.

[29] E. W. Lemmon, I. H. Bell, M. L. Huber, and M. O. McLinden, in *NIST Chemistry WebBook*, NIST Standard Reference Database, Vol. 69, edited by P. J. Linstrom and W. G. Mallard (National Institute of Standards and Technology, 2022) Chap. Thermophysical Properties of Fluid Systems.

[30] V. K. Sharma, S. Bhagour, D. Sharma, and S. Solanki, Thermochimica Acta **563**, 72 (2013).

[31] D. Groom, in *Review of Particle Physics*, edited by R. Workman *et al.* (Particle Data Group, 2021) Chap. Atomic and Nuclear Properties, to be published (2022), https://pdg.lbl.gov/2022/AtomicNuclearProperties/.

[32] M. Inui, D. Ishikawa, K. Matsuda, K. Tamura, S. Tsutsui, and A. Baron, Journal of Physics and Chemistry of Solids **66**, 2223 (2005), 5th International Conference on Inelastic X-ray Scattering (IXS 2004).

[33] R. Singh, S. Arafin, and A. George, Physica B: Condensed Matter **387**, 344 (2007).

[34] F. Habashi, Mercury, physical and chemical properties, in *Encyclopedia of Metalloproteins*, edited by R. H. Kretsinger, V. N. Uversky, and E. A. Permyakov (Springer New York, New York, NY, 2013) pp. 1375–1377.

[35] L. A. Davis and R. B. Gordon, The Journal of Chemical Physics **46**, 2650 (1967), https://doi.org/10.1063/1.1841095.

[36] R. V. G. Rao and S. K. Dutta, Zeitschrift für Physikalische Chemie **264O**, 771 (1983).

[37] E. W. Lemmon and R. T. Jacobsen, International Journal of Thermophysics **25**, 21 (2004).

[38] C. Tegeler, R. Span, and W. Wagner, Journal of Physical and Chemical Reference Data **28**, 779 (1999), https://doi.org/10.1063/1.556037.

[39] R. Span, E. W. Lemmon, R. T. Jacobsen, W. Wagner, and A. Yokozeki, Journal of Physical and Chemical Reference Data **29**, 1361 (2000), https://doi.org/10.1063/1.1349047.

[40] E. W. Lemmon and R. Span, Journal of Chemical & Engineering Data **51**, 785 (2006), https://doi.org/10.1021/je050186n.

[41] M. Huber, Models for viscosity, thermal conductivity, and surface tension of selected pure fluids as implemented in refprop v10.0 (2018).

[42] R. M. Sternheimer, Methods in Experimental Physics **5**, 1 (1961).

[43] C. Amsler, in *REVIEW OF PARTICLE PHYSICS*, Vol. 1 (Particle Data Group, 2010) pp. 411–450.

[44] P. Oikonomou, F. Arneodo, and L. Manenti, GitHub Repository doi:https://github.com/PanosEconomou/LXe-Phonon (2021).